

**Table 3** VALUES OF  $A_{min}$  AT INTERPOLATION POINTS

$x_0 y_0 z_0$ : 22.2 V	$x_1 y_0 z_1$ : 8.5 V
$x_1 y_0 z_0$ : 19.5 V	$x_0 y_1 z_1$ : 8.9 V
$x_0 y_1 z_0$ : 19.0 V	$x_2 y_0 z_0$ : 17.2 V
$x_0 y_0 z_1$ : 12.0 V	$x_0 y_2 z_0$ : 15.0 V
$x_1 y_1 z_0$ : 15.7 V	$x_0 y_0 z_2$ : 9.0 V

nomial of second degree in three variables:

$$\begin{aligned}
 P_2(x,y,z) = & 22.2 + 2.88(z - z_0) - 0.32(z - z_0)(z - z_1) \\
 & + 76.2(y - y_0) + 0.67(y - y_0)(z - z_0) \\
 & + 35.7(y - y_0)(y - y_1) + 0.71(x - x_0) \\
 & - 0.052(x - x_0)(z - z_0) - 3.74(x - x_0)(y - y_0) \\
 & - 0.0011(x - x_0)(x - x_1)
 \end{aligned}$$

The validity of this polynomial as a model for  $A_{min}$  was questioned in two different situations, namely:

(a) if the polynomial is evaluated at points far from the interpolation points within the tolerance region

(b) if  $A_{min}$  is predicted in the sweep generator of another TV receiver. In this case all components apart from  $x, y, z$  would be randomly different within nominal tolerances.

To validate case (a), measurements were performed with the original circuit, circuit no. 1, at three points far from the interpolation region.

To validate case (b),  $A_{min}$  was measured in another TV receiver, circuit no. 2, at five interpolation points identical to those selected for the original circuit.

A comparison between experimental values of  $A_{min}$  and predicted values with the polynomial showed a difference smaller than 1 V in all cases considered above. This accuracy was considered fairly good to describe the value of  $A_{min}$  in this circuit.

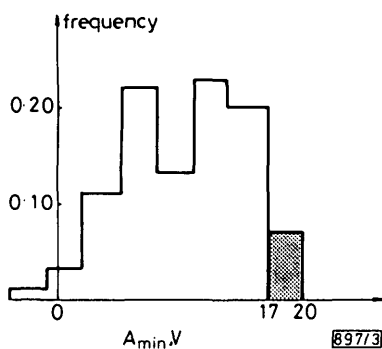


**Fig. 3** Histogram of  $A_{min}$

A Monte Carlo simulation was performed using the polynomial, and the histogram of  $A_{min}$  obtained is shown in Fig. 3. Since values of  $A_{min}$  greater than 17 V imply parametric failures of the circuit, it can be seen that 7% of the circuits would fail.

**Conclusions:** The output voltage of a series regulator and the synchronising pulse requirement of a TV sweep generator were adequately modelled for statistical simulation by Newton's interpolation polynomials.

A circuit simulation program or experimental measurements are required at a few interpolation points, but the Monte Carlo run can be done with the polynomial alone, thereby saving considerable computer time.

Since the theory of multivariate approximating functions is currently of great interest, doubtless better approaches can be found.

R. AMADOR  
R. LÓPEZ

28th March 1984

Laboratorio de Microelectrónica  
Instituto Superior Politécnico J. A. Echeverría  
Apartado 8016  
Ciudad Habana 8, Cuba

## References

- 1 BALABAN, P., and GOLEMBESKI, J.: 'Statistical analysis for practice circuit design', *IEEE Trans.*, 1975, **CAS-22**
- 2 BALABANIAN, N.: 'Synthesis of active RC networks'. Revista Comunicaciones, 1970, Havana, Cuba (in Spanish)
- 3 ISAACKSON, E., and KELLER, H. B.: 'Analysis of numerical methods' (Wiley, 1966)

## ACCURATE ANALYTICAL METHOD FOR THE EXTRACTION OF SOLAR CELL MODEL PARAMETERS

*Indexing term: Solar cells*

Analytical expressions are derived for the rapid extraction of solar cell single diode model parameters from experimental data. The resulting parameter values are shown to have less than 5% error for most solar cells.

The determination of solar cell model parameters from experimental data is important in the design and evaluation of solar cells. Whilst a number of methods have been suggested for measuring the series resistance of a solar cell,<sup>1-4</sup> other parameters, which are also important, have not received the same amount of attention, and no rapid and accurate methods of extracting these other parameters have so far been proposed.

The single diode lumped parameter equivalent circuit of a solar cell is given in Fig. 1. At a given illumination, the current/voltage relationship is given by

$$I = I_{ph} - \left( \frac{V + IR_s}{R_{sh}} \right) - I_s \left( \exp \frac{V + IR_s}{nV_T} - 1 \right) \quad (1)$$

It has been shown<sup>5</sup> that the circuit parameters  $R_s$ ,  $R_{sh}$ ,  $I_s$  and  $n$  at a particular temperature and illumination can be computed from the values  $V_{oc}$ ,  $I_{sc}$ ,  $V_m$ ,  $I_m$ ,  $R_{so}$  and  $R_{sho}$  measured from the  $I/V$  characteristic, where  $V_{oc}$  = open-circuit voltage,  $I_{sc}$  = short-circuit current,  $V_m$  = voltage at the maximum power point,  $I_m$  = current at the maximum power point,

$$R_{so} = - \left( \frac{dV}{dI} \right)_{V=V_{oc}} \quad (2)$$

$$R_{sho} = - \left( \frac{dV}{dI} \right)_{I=I_{sc}} \quad (3)$$

It has also been shown<sup>5</sup> that the lumped circuit parameters can be evaluated from the following nonlinear equations:

$$I_s \left( \exp \frac{V_{oc}}{nV_T} - \exp \frac{I_{sc} R_s}{nV_T} \right) - I_{sc} \left( 1 + \frac{R_s}{R_{sh}} \right) + \frac{V_{oc}}{R_{sh}} = 0 \quad (4)$$

$$(R_{so} - R_s) \left( \frac{1}{R_{sh}} + \frac{I_s}{nV_T} \exp \frac{V_{oc}}{nV_T} \right) - 1 = 0 \quad (5)$$

$$\frac{1}{R_{sh}} - \frac{1}{R_{sho} - R_s} + \frac{I_s}{nV_T} \exp \frac{I_{sc} R_s}{nV_T} = 0 \quad (6)$$

$$\begin{aligned}
 I_s \exp \frac{V_{oc}}{nV_T} + \frac{V_{oc} - V_m}{R_{sh}} - \left( 1 + \frac{R_s}{R_{sh}} \right) I_m \\
 - I_s \exp \frac{V_m + R_s I_m}{nV_T} = 0
 \end{aligned} \quad (7)$$

Kennerud<sup>5</sup> and Charles *et al.*<sup>6</sup> have shown that the four parameters  $n$ ,  $I_s$ ,  $R_s$  and  $R_{sh}$  may be determined by using the Newton-Raphson method of solving the nonlinear simultaneous eqns. 4-7. However, this method requires extensive

computation and also good initial guesses for the iterations to converge. In many cases, it was found that there are difficulties in determining these guesses in order to solve the equations.<sup>7</sup> Thus there is a need for analytical expressions that will enable the direct determination of  $I_{ph}$ ,  $n$ ,  $I_s$ ,  $R_s$  and  $R_{sh}$ .

Consider the following typical parameters for a 3" solar cell under AM1 illumination:  $I_{ph} = 1.0$  A,  $R_s = 0.05$   $\Omega$ ,  $R_{sh} = 500$   $\Omega$ ,  $I_s = 10^{-7}$  A,  $n = 1.3$ ,  $V_{oc} = 0.545$  V,  $I_{sc} = 1.0$  A,  $R_{so} = 0.0838$   $\Omega$ ,  $R_{sho} = 497$   $\Omega$ ,  $V_m = 0.415$  V,  $I_m = 0.916$  A,  $T = 27^\circ\text{C}$  and  $FF = 0.698$ .

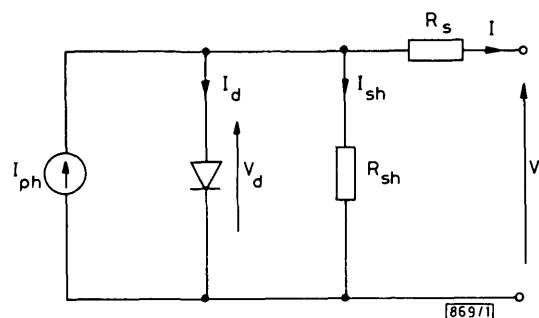


Fig. 1 Single diode model for solar cells

$$I_d = I_s \exp\left(\frac{V_d}{nV_T} - 1\right)$$

By substituting these values into eqn. 4, it is evident that  $\exp(V_{oc}/nV_T)$  is much greater than  $\exp(I_{sc}R_s/nV_T)$ . The term  $I_s \exp(I_{sc}R_s/nV_T)$  may therefore be neglected provided the illumination is such that  $I_{ph}$  is less than 10 A (i.e. equivalent to illumination of less than 10 suns) for less than 10% error. Also, since  $R_s \ll R_{sh}$ ,  $1 + (R_s/R_{sh})$  may be written as 1. For the typical values cited above, in eqn. 5 the term  $(I_s/nV_T) \times \exp(V_{oc}/nV_T)$  is much greater than  $1/R_{sh}$ , and in eqn. 6 the term  $(I_s/nV_T) \exp(I_{sc}R_s/nV_T)$  is much less than 10% of the other terms provided  $I_{ph}$  is less than 6 A (i.e. illumination less than 6 suns at AM1).

After ignoring the terms that may be neglected we obtain the following:

$$I_s \exp\left(\frac{V_{oc}}{nV_T}\right) - I_{sc} + \frac{V_{oc}}{R_{sh}} = 0 \quad (8)$$

$$(R_{so} - R_s) \frac{I_s}{nV_T} \exp\left(\frac{V_{oc}}{nV_T}\right) - 1 = 0 \quad (9)$$

$$R_{sh} = R_{sho} \quad (10)$$

$$I_s \exp\left(\frac{V_{oc}}{nV_T}\right) + \frac{V_{oc} - V_m}{R_{sh}} - I_m - I_s \exp\left(\frac{V_m + R_s I_m}{nV_T}\right) = 0 \quad (11)$$

From these equations an analytical expression for  $n$  in terms of the measured parameters is

$$n = \frac{V_m + R_{so} I_m - V_{oc}}{V_T \left\{ \ln\left(I_{sc} - \frac{V_m}{R_{sho}} - I_m\right) - \ln\left(I_{sc} - \frac{V_{oc}}{R_{sh}}\right) + \frac{I_m}{I_{sc} - (V_{oc}/R_{sho})} \right\}} \quad (12)$$

$I_s$ ,  $R_s$  and  $I_{ph}$  may then be found from:

$$I_s = \left(I_{sc} - \frac{V_{oc}}{R_{sh}}\right) \exp\left(-\frac{V_{oc}}{nV_T}\right) \quad (13)$$

$$R_s = R_{so} - \frac{nV_T}{I_s} \exp\left(-\frac{V_{oc}}{nV_T}\right) \quad (14)$$

$$I_{ph} = I_{sc} \left(1 + \frac{R_s}{R_{sh}}\right) + I_s \left(\exp\left(\frac{I_{sc} R_s}{nV_T}\right) - 1\right) \quad (15)$$

Thus, all the parameters of the single diode model can be found from eqns. 10, 12, 13, 14 and 15.

Table 1 COMPARISON OF PARAMETERS EXTRACTED BY ANALYTICAL EXPRESSIONS AND ITERATIVE METHOD FOR TWO EXPERIMENTAL CELLS

Experimental data	Blue cell	Grey cell
$V_{oc}$ , V	0.536	0.524
$I_{sc}$ , A	0.1023	0.561
$V_m$ , V	0.437	0.390
$I_m$ , A	0.0925	0.481
$R_{so}$ , $\Omega$	0.45	0.162
$R_{sho}$ , $\Omega$	1000	25.9
$T$ , K	300	307

Results	Iterative	Analytical	Iterative	Analytical
$I_{ph}$ , A	0.1023	0.1023	0.5627	0.5610
$n$	1.5017	1.5019	1.7168	1.7225
$I_s$ , $\mu A$	0.1034	0.1036	5.326	5.514
$R_s$ , m $\Omega$	68.51	68.26	78.52	77.69
$R_{sh}$ , $\Omega$	1003.1	1000.0	26.03	25.9

The errors present in the analytical expressions in eqns. 10, 12–14 were computed. These errors introduced by the assumptions incorporated in the derivation of the analytical expressions were computed as follows. A theoretical  $I/V$  characteristic was computed from the model using base values of  $I_{ph} = 1$  A,  $I_s = 10^{-7}$  A and  $n = 1.3$  and different combinations of  $R_s$  and  $R_{sh}$ .  $R_s$  was varied in the range 1 m $\Omega$  to 1  $\Omega$  and  $R_{sh}$  was varied in the range 10  $\Omega$  to 10 k $\Omega$ . The parameters were recovered from the characteristic using the analytical expressions and compared with the actual values used in generating the characteristic. The differences were expressed in terms of percentage errors and plotted in a grid of  $R_s$  and  $R_{sh}$  values. The results are presented in Fig. 2, where the 1% and 5% error contours for parameters  $n$ ,  $I_s$ ,  $R_s$  and  $R_{sh}$  are drawn in an  $R_s - R_{sh}$  grid. The results in Fig. 2 show that the analytical expressions for all four parameters are accurate to within 1% provided  $R_s$  is in the range 1 m $\Omega$  to 150 m $\Omega$  and  $R_{sh}$  is in the range 30 to 3000  $\Omega$ . For 5% errors, the range of validity is even wider, and would include most solar cells.

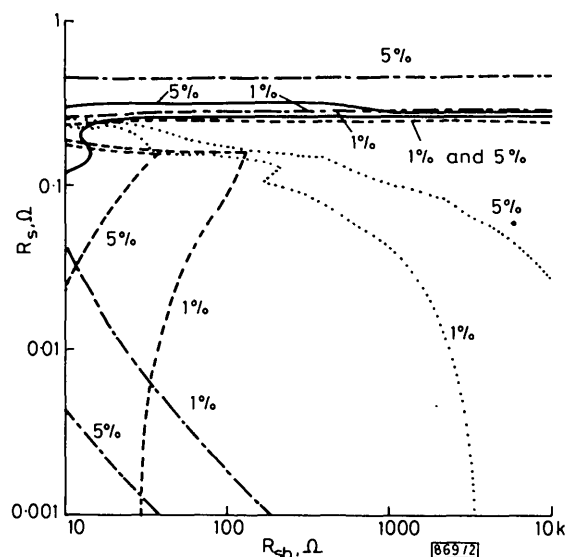


Fig. 2 Error contours of extracted parameters

—  $n$  error  
 ---  $I_s$  error  
 -.-  $R_s$  error  
 .....  $R_{sh}$  error

The model parameters of two cells of differing quality were extracted using these analytical expressions and compared with parameters extracted using the iterative method.<sup>5</sup> The experimental data (taken from Charles *et al.*<sup>6</sup>) and the results are set out in Table 1. It can be seen that the results obtained by the two methods are virtually identical for the high-quality 'blue' cell, and differ by no more than 4% for the lower-quality

'grey' cell. These results together with the error contours effectively demonstrate that the analytical expressions enable the rapid and accurate determination of lumped circuit parameters for most solar cells.

J. C. H. PHANG  
D. S. H. CHAN  
J. R. PHILLIPS

22nd March 1984

Department of Electrical Engineering  
National University of Singapore  
Kent Ridge, Singapore 0511

## References

- 1 WOLF, M., and RAUSCHENBACH, H.: 'Series resistance effects on solar cell measurements', *Adv. Energy Conversion*, 1963, 3, pp. 455-479
- 2 PHANG, J. C. H., and CHAN, D. S. H.: 'Comments on the experimental determination of series resistance in solar cells', *IEEE Trans.*, ED (to be published)
- 3 RAJAKANAN, K., and SHEWCHUN, J.: 'A better approach to the evaluation of the series resistance of solar cells', *Solid State Electron.*, 1979, 22, pp. 193-197
- 4 ARAUJO, G. L., and SANCHEZ, E.: 'A new method for experimental determination of the series resistance of a solar cell', *IEEE Trans.*, 1982, ED-29, pp. 1511-1513
- 5 KENNERUD, K. L.: 'Analysis of performance degradation in CdS solar cells', *ibid.*, 1969, AES-5, pp. 912-917
- 6 CHARLES, J. P., ABDELKRIM, M., MUOY, Y. H., and MIALHE, P.: 'A practical method of analysis of the current-voltage characteristics of solar cells', *Sol. Cells*, 1981, 4, pp. 169-178
- 7 BRAUNSTEIN, A., BANY, J., and APPELBAUM, J.: 'Determination of solar equation parameters from empirical data', *Energy Conversion*, 1977, 17, pp. 1-6

## IN-THE-LENS SECONDARY ELECTRON ANALYSER FOR IC INTERNAL VOLTAGE MEASUREMENTS WITH ELECTRON BEAMS

Indexing terms: Integrated circuits, Electron microscopy

A new analyser scheme for voltage measurements on integrated circuits (ICs) can be performed using a secondary electron (SE) analyser and a finely focused electron beam which acts as a contactless, nonloading, easily positionable probe.

Quantitative voltage measurements on integrated circuits (ICs) can be performed using a secondary electron (SE) analyser and a finely focused electron beam which acts as a contactless, nonloading, easily positionable probe.

This analyser has to fulfil three functions: (i) provide an extraction field to eliminate the measurement accuracy degradation due to the influences of microfields on the IC surface; (ii) provide a retarding field that analyses the SE energy; (iii) provide a deflection unit that deflects the SEs towards a detector.

In a conventional scanning electron microscope (SEM), which generates and controls the electron probe, the energy analyser is located between the bottom of a 'pinhole' objective lens and the IC. In this arrangement the analyser limits the minimum working distance (i.e. distance between the bottom of the objective lens and IC surface) to about 12-25 mm. This in turn compromises the probe-forming capability of the electron optical system, as the shorter the working distance, the higher the probe current density, and the better the spatial resolution of the arrangement. The voltage resolution of the analyser, on the other hand, improves as the spacing between the extraction and analyser grids increases, which can only be accomplished by lengthening the analyser. These conflicting requirements necessitate a compromise in terms of spatial and voltage resolution to be struck.

Using an ISI model SS-60 SEM, which employs an open-bore objective lens, with SE detection above the lens, a new analyser scheme has been developed that overcomes the trade-offs between spatial and voltage resolution.

Fig. 1 shows a schematic diagram of the new analyser scheme, compared to the below-the-lens arrangement used until now. Primary electrons (PE) pass through a series of grids or apertures and generate SEs at the IC surface, which is located typically 3 mm below the objective lens. This short working distance allows the achievement of 3-5 times smaller beam probes, containing the same current as is possible at 25 mm working distance.

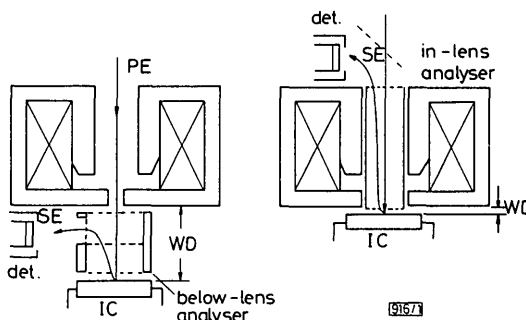


Fig. 1 Comparison between below- and in-lens analysers

The SEs are accelerated by the extraction field and enter the retarding region. Planar equipotential lines parallel to the grid planes are assured by a resistive coating on the inner wall of the analyser. All SEs with energies larger than the retarding voltage enter the deflection region and are detected by the SE detector.

Applying a ramp signal to the retarding grid yields the integral SE spectral distribution, or 'S-curve', which is shifted when voltages are applied to the specimen. The voltage measurement is performed by analysing this S-curve shift. High-accuracy measurements are possible only if the S-curve shape remains constant with applied specimen voltage. This is the case for the in-the-lens analyser as demonstrated in Fig. 2.

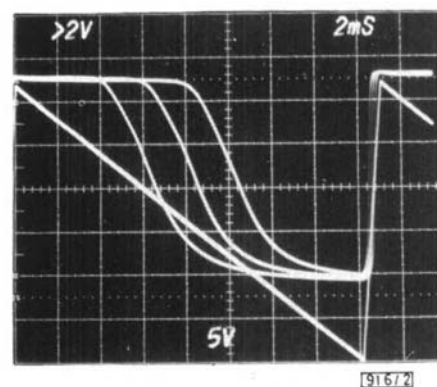


Fig. 2 S-curves taken at  $V_{extr} = 1.5$  kV and specimen voltages of +4 V (left curve), 0 V (centre curve) and -4 V (right curve)

The ramp signal applied to the retarding grid varies from +12 to -20 V

The voltage resolution  $\Delta V$  of SE analysers is given by

$$\Delta V = nC[T, \Delta E/E, V_{ret}, N(E)](\Delta f/I_{pe})^{1/2}$$

where  $n$  is the acceptable signal/noise ratio on the detected signal, and  $C$  is a factor which depends on the transmission  $T$ , the analyser energy resolution  $\Delta E/E$ , the retarding voltage  $V_{ret}$  and the spectrum of the SEs, given by  $N(E)$ .  $\Delta f$  = system bandwidth and  $I_{pe}$  = primary electron beam current. The factor  $C$  on an aluminium surface was determined to be  $6 \times 10^{-9} \text{ V(As)}^{1/2}$  at  $V_{extr} = 500$  V, and  $8 \times 10^{-9} \text{ V(As)}^{1/2}$  at  $V_{extr} = 1500$  V. The factor  $C$  for the in-the-lens analyser is more than 20 times smaller than achieved by below-the-lens analysers<sup>1</sup> and reduces the measurement (integration) time for a given voltage resolution by a factor of about 5.

The energy resolution  $\Delta E/E$  was measured by simulating SEs with a low energy electron gun with low energy spread of